LAWRENCE
LIVERMORE
NATIONAL
LABORATORY

UCRL-JRNL-218397

Phonon Density of States and Sound Velocities of Magnesiowüstite in Earth's Lower Mantle

J.-F. Lin, S. D. Jacosben, W. Sturhahn, J. Jackson, J. Zhao, C.-S. Yoo

January 25, 2006

Geophysical Research Letters

Phonon Density of States and Sound Velocities of Magnesiowüstite in Earth's Lower Mantle

Jung-Fu Lin[*], Steven D. Jacobsen[†], Wolfgang Sturhahn[§], Jennifer M. Jackson[†], Jiyong Zhao[§], Choong-Shik Yoo[*]

[*]*Lawrence Livermore National Laboratory, 7000 East Avenue, Livermore, CA 94550*
[†]*Geophysical Laboratory, Carnegie Institution of Washington, 5251 Broad Branch Rd. NW, Washington, DC 20015*
[§]*Advanced Photon Source, Argonne National Laboratory, 9700 South Cass Avenue, Argonne, IL 60439*

Corresponding author and requests for materials should be addressed to:
Jung-Fu Lin, Lawrence Livermore National Laboratory, 7000 East Avenue, L-415
Livermore, CA 94550, Tel: (925) 4244157, Fax: (925) 422-6594, Email: lin24@llnl.gov

The partial phonon densities of states of iron in magnesiowüstite [$(Mg_{0.75},Fe_{0.25})O$] have been measured by nuclear inelastic X-ray scattering up to 109 GPa. Compressional and shear wave velocities, shear moduli, and their pressure derivatives increase significantly across the spin-pairing transition of iron in $(Mg_{0.75},Fe_{0.25})O$ at approximately 50 GPa. The effects of the transition on the elastic properties of (Mg,Fe)O at lower-mantle pressures are in contrast to what was predicted by studying MgO and high-spin magnesiowüstite, and need to be considered in future geophysical modeling of the lower mantle. The transition also affects other thermodynamic properties of magnesiowüstite under high pressures.

The transition metal oxide (Mg,Fe)O (magnesiowüstite) is thought to be the second most abundant mineral in the Earth's lower mantle after silicate perovskite, aluminous $(Mg,Fe)SiO_3$ [1-13]. Pressure-induced electronic spin-pairing transitions of iron in magnesiowüstite have been predicted by theoretical calculations [1] and detected by X-ray emission spectroscopy [5,8], Mössbauer spectroscopy [10,13], and X-ray diffraction [8,11]. These studies indicate that an isosymmetric spin-pairing transition from a paramagnetic high-spin state to a diamagnetic low-spin state occurs in MgO-rich magnesiowüstite, and that addition of iron into MgO stabilizes the high-spin state to higher pressures [13]. The electronic spin-pairing transition in (Mg,Fe)O may terminate at a critical temperature [9], widening the spin transition to a more gradual spin crossover over an extended pressure range at high temperatures. Since magnesiowüstite constitutes a considerable volume fraction of the lower mantle (~10-20%), an understanding of the effects of the electronic spin-pairing transition on the thermoelastic and transport properties of (Mg,Fe)O is crucial to modeling deep-Earth geodynamics and geochemistry

[2,7]. A recent X-ray diffraction study of $(Mg_{0.83},Fe_{0.17})O$ to 135 GPa showed a dramatic jump in the isothermal bulk modulus (K_T) and bulk sound velocity (V_Φ) at the spin-paring transition [8], but compressional (V_P) and shear (V_S) wave velocities and shear modulus (G) of the low-spin magnesiowüstite have not previously been measured. Here we have determined the partial phonon densities of states (PDOS) of iron in $(Mg_{0.75},Fe_{0.25})O$ by nuclear resonant inelastic X-ray scattering (NRIXS) up to 109 GPa. NRIXS using a high-intensity synchrotron X-ray source probes the PDOS for ^{57}Fe incorporated into ^{57}Fe-bearing samples [14], and has been used with a diamond-anvil cell (DAC) to determine the elastic, thermodynamic, and vibrational properties of ^{57}Fe-containing materials at high pressure [15-19]. We have derived the elastic, thermodynamic, and vibrational properties of $(Mg_{0.75},Fe_{0.25})O$ from the PDOS, including V_P, V_S, and G. These properties are used to understand the effects of the electronic spin-pairing transition on the physical properties of magnesiowüstite in the Earth's lower mantle.

High-pressure NRIXS experiments were conducted at sector 3 of the Advanced Photon Source (APS), Argonne National Laboratory (ANL) [14,20]. Energy spectra were obtained by tuning the X-ray energy ($\pm$70 meV to $\pm$90 meV in steps of 0.25 meV) around the nuclear transition energy of 14.4125 keV with an energy resolution of 1 meV. The Fe-$K_{\alpha,\beta}$ fluorescence radiation, emitted with time delay relative to the incident X-ray pulses, was collected by three avalanche photodiode detectors. The counting time for each NRIXS spectrum was approximately one hour, and ten to twenty spectra were collected and added at each pressure.

A quasiharmonic model was used to extract the PDOS from the measured energy spectra (Fig. 1) [14]. While the integration of the PDOS gives the elastic, thermodynamic, and vibrational parameters from the contribution of the iron atoms in

$(Mg_{0.75},Fe_{0.25})O$, the bulk Debye sound velocity (V_D) of the sample is derived from parabolic fitting of the low-energy slope of the PDOS in the range of approximately 0.2 meV to 15 meV after applying a correction factor, the cube root of the ratio of the mass of the nuclear resonant isotope (^{57}Fe) to the average atomic mass of the sample [16]. The procedure of deriving V_P, V_S, and G from the V_D and equation of state (EOS) parameters, namely the adiabatic bulk modulus (K_S) and density (ρ), has been described previously [14-16,18,20]. Here we used the EOS parameters for the high-spin and low-spin magnesiowüstite from a recent X-ray diffraction study [8] using Birch-Murnaghan EOS [21]; the K_S and its pressure derivative of MgO with the density of $(Mg_{0.75},Fe_{0.25})O$ was also used to calculate the V_P, V_S, and G for the low-spin magnesiowüstite and to understand the potential influence of the input EOS on the derived parameters [22,23], because a separate X-ray diffraction study indicates that the compression curves of the low-spin phases in various (Mg,Fe)O compositions are identical to that of MgO [11]. The NRIXS technique is particularly well suited for constraining V_S and G from a precise measurement of V_D because they are considerably less sensitive to the choice of EOS input data (K_S, ρ) compared with V_P [18] (Fig. 2). Under ambient conditions, our V_P, V_S, and G values are consistent with previous ultrasonic measurements [3] (Fig. 2), verifying the procedure for deriving sound velocities from PDOS. Compared with MgO [23], addition of 25 atom% FeO into MgO significantly reduce the value of V_P, V_S, and G for the high-spin magnesiowüstite, while the value of K_S is unchanged within experimental uncertainties, consistent with recent high-pressure ultrasonic and Brillouin studies [3,4,6,7,12]. An abnormal behavior in the elastic, thermodynamic, and vibrational properties in $(Mg_{0.75},Fe_{0.25})O$ occurs between 42 GPa and 62 GPa (Fig. 2-3). The high-pressure low-spin magnesiowüstite exhibits a much higher V_P, V_S, and G than the low-

pressure high-spin magnesiowüstite (Fig. 2). An additional important observation is that there is a significant increase in the pressure derivatives of the V_P, V_S, and G for the low-spin magnesiowüstite, as compared to the high-spin magnesiowüstite.

The electronic spin-pairing transition of iron are also found to significantly influence other elastic, thermodynamic and vibrational properties of $(Mg_{0.75},Fe_{0.25})O$ (Fig. 3); the mean force constant (D_{av}), Lamb-Mössbauer factor (f_{LM}), kinetic energy (E_k), and kinetic energy at 0 K (E_z) all increase while vibrational specific heat (C_{vib}) and vibrational entropy (S_{vib}) decrease across the electronic transition at ~50 GPa [20]. The observed increase in the D_{av} and f_{LM} across the transition are, in general, consistent with the increase in the K_S reported by a recent X-ray diffraction study [8]. The K_S can be attributed from two main factors, the interatomic force constant and the electronic contribution, where the interatomic force constant is directly related to the D_{av} through [17,24]:

$$\frac{M}{\sqrt[3]{V}}\sum_i \frac{\overline{D}_i}{2} \qquad (1)$$

where V is the volume of a polyhedra, M is a constant determined by the geometry of the polyhedra, and i indicates an atom in the polyhedra. Assuming the change in M is small across the transition [17] and scaling the D_{av} with the cube root of the unit cell volume of $(Mg_{0.75},Fe_{0.25})O$ (see equation 1), the observed increase in the D_{av} across the spin-pairing transition indicates an increase in the interatomic force constant and hence the observed jump in the bulk modulus. On the other hand, the electronic contribution to the bulk modulus should be negligible because magnesiowustite is most likely an insulator across the transition. The Lamb-Mössbauer factor (f_{LM}), is related to the mean square displacement ($<u^2>$) by

$$f_{LM} = e^{-k^2\langle u^2\rangle} \quad (2)$$

where k is the wavenumber of the absorbed X-ray photon [14]. Therefore, an increase in the f_{LM} indicates a much reduced displacement of iron atoms and stiffening in the low-spin $(Mg_{0.75},Fe_{0.25})O$ (Fig. 3), also consistent with the increase in G and K_S across the transition.

The dramatic effects of the spin transition of iron on the elastic and thermodynamic properties of magnesiowustite reported here have important implications for the geophysics of the Earth's lower mantle [1,7,25-28], first-principle theoretical calculations [29], and electronic spin-pairing transitions in other transition metal oxide systems [30,31]. Measurements of the sound velocities and elasticity of magnesiowüstite and silicate perovskite, the most abundant mineral assemblage of the lower mantle, under high pressures and/or high temperatures have been used to relate seismic observations in Earth's lower mantle and to infer its mineralogy and chemistry; however, these studies for magnesiowüstite were often limited to the high-spin state [2,7,25-29]. Comparison between the V_P and V_S of the lower mantle and that of the synthetic pyrolite model [26,27] with silicate perosvkite and magnesiowustite under high pressures and temperatures has shown that the pressure derivatives of the V_P and V_S of these minerals, including magnesiowustite, are too high to match the seismic model of the lower mantle toward the deep lower mantle below 60 to 70 GPa (approximately 1500 km in depth); these systematic deviations cannot be accounted for by temperature effects alone [7,27-29]. Although the nature of the electronic spin-pairing transition under Earth's mantle conditions have yet to be understood experimentally, recent theoretical predictions suggest that the transition in magnesiowüstite would occur over an extended pressure

range of approximately 30 GPa (or ~700 km in depth) [9]. In this case, the associated increase in the V_P, V_S, G, K_S, and their pressure derivatives across a gradual spin crossover in magnesiowüstite would further gradually increase the mismatch between the synthetic pyrolite model and PREM. That is, a stronger radial inhomogeneity in the deeper part of the lower mantle would be needed to account for the mismatch [32,33]. The effects of the transition on the elastic properties of (Mg,Fe)O at lower-mantle pressures are in contrast to what was predicted by studying pure MgO and high-spin magnesiowüstite, and may reconcile observed seismic heterogeneity and possible compositional layering in Earth's lower mantle. It also remains to be seen how high temperature affects the elastic, thermodynamic, and transport properties of the low-spin magnesiowüstite under lower mantle conditions, but the emerging picture of the Earth's deeper mantle from the presence of the most abundant transition metal, iron, in magnesiowüstite and the associated effects on the thermoelastic properties across the electronic spin-pairing transition indicates that previous models of lower-mantle velocities from mineral physics data using pure MgO or (Mg,Fe)O containing high-spin Fe are insufficient to correctly model the behavior of this abundant phase in the lower mantle. Therefore, the dramatic effects of the spin transition on the elastic and thermodynamic properties of (Mg,Fe)O need to be taken into account in future geophysical and geochemical models of the Earth's complex lower mantle.

1. D. M. Sherman, *J. Geophys. Res.* **96**, B9, 14299 (1991).

2. I. Jackson, *Geophys. J. Int.* **134**, 291 (1998).

3. S. D. Jacobsen *et al.*, *J. Geophys. Res.* **107**, B2, 10.1029/2001JB000490 (2002).

4. J. Kung, B. Li, D. J. Weidner, J. Zhang, R. C. Liebermann, *Earth Planet. Sci. Lett.* **203**, 557 (2002).

5. J. Badro *et al*., *Science* **300,** 789 (2003).

6. S. D. Jacobsen, H. Spetzler, H. J. Reichmann , J. R. Smyth, *Proc. Natl. Acad. Sci.* **100**, 5867 (2004).

7. J. M. Jackson, The effect of minor elements on the physical and chemical properties of lower mantle minerals at high pressure (University of Illinois at Urbana-Champaign, 2005), pp. 98.

8. J. F. Lin *et al.*, *Nature* **436**, 377 (2005).

9. W. Sturhahn, J. M. Jackson, J. F. Lin, *Geophys. Res. Lett.* **32**, L12307 (2005).

10. S. Speziale *et al.*, *Proc. Natl. Acad. Sci.* **102**, 17918 (2005).

11. Y. Fei *et al.*, *Eos Trans. AGU, Fall Meet. Suppl.* **86(52)**, MR14A-05 (2005).

12. J. M. Jackson *et al.*, submitted to *J. Geophys. Res.* (2006).

13. J. F. Lin *et al.*, submitted to *Phys. Rev. Lett.* (2006).

14. W. Sturhahn, *J. Phys.: Condens. Matter* **16,** S497 (2004).

15. H. K. Mao *et al.*, *Science* **292**, 914 (2001).

16. M. Hu *et al.*, *Phys. Rev. B* **67**, 094304 (2003).

17. H. Kobayashi *et al.*, *Phys. Rev. Lett.* **93**, 195503 (2004).

18. W. Mao *et al.*, *Geophys. Res. Lett.* **31**, L15618 (2004).

19. J. F. Lin *et al.*, *Science* **308**, 1892 (2005).

20. Materials and Methods are available as supporting material on *Science* Online.

21. F. Birch, *J. Geophys. Res.* **91**, 4949 (1986).

22. G. F. Davies, A. M. Dziewonski, *Phys. Earth Planet. Int.* **10**, 336 (1975).

23. C. S. Zha, H. K. Mao, R. J. Hemley, *Proc. Natl. Acad. Sci.* **97**, 13494 (2000).

24. G. Kotliar, S. Murthy, M. J. Rozenberg, *Phys. Rev. Lett.* **89**, 046401 (2002).

25. A. M. Dziewonski, D. L. Anderson, *Phys. Earth Planet. Inter.* **25**, 297 (1981).

26. A. E. Ringwood, *J. Geology* **90**, 611 (1982).

27. E. Mattern, J. Matas, Y. Ricard, J. Bass, *Geophys. J. Int.* **160**, 973 (2005).

28. B. Li, J. Zhang, *Phys. Earth Planet. Inter.* **151**, 143 (2005)

29. R. M. Wentzcovitch, B. B. Karki, M. Cococcioni, S. de Gironcoli, *Phys. Rev. Lett.* **92**, 018501 (2004).

30. M. F. Mott, *Metal Insulator Transitions* (Tayor and Francis, London, 1990), pp. 286.

31. R. E. Cohen, I. I. Mazin, D. G. Isaak, *Science* **275**, 654 (1997).

32. L. H. Kellogg, B. H. Hager, R. D. van der Hilst, *Science* **283**, 1881 (1999).

33. R. D. van der Hilst, H. Kárason, *Science* **283**, 1885 (1999).

34. We acknowledge XOR-3, APS, ANL for the use of the synchrotron facilities and HPCAT for the use of the ruby system. We thank V. V. Struzhkin, Y. Fei, V. Iota, and H. C. Cynn for their fruitful discussions. We wish to thank E. E. Alp for designing the new Be gaskets. This work and use of the APS are supported by U.S. DOE, Basic Energy Sciences, Office of Science, under contract No. W-31-109-ENG-38, and the State of Illinois under HECA. This work at LLNL was performed under the auspices of the U.S. DOE by University of California and LLNL under Contract No. W-7405-Eng-48. J.F.L. is also supported by the Lawrence Livermore Fellowship. S.D.J. acknowledges financial support from NSF-EAR 0440112 and a Carnegie Fellowship.

Figure Captions:

Fig. 1. PDOS of $(Mg_{0.75},Fe_{0.25})O$ under high pressures. The spectral features of PDOS are shifted to higher energies with increasing pressure, whereas the energy shift is much more significant across the electronic spin-pairing transition from 42 to 62 GPa. The low-energy slope of the PDOS in the range of 0.2 meV to 15 meV is used to derive the bulk Debye sound velocity (V_D) [14,16].

Fig. 2. Comparison of aggregate V_P (A), V_S (B), and G (C) of $(Mg_{0.75},Fe_{0.25})O$ at high pressures. Open circles: this study based on the Birch-Murnaghan EOS [21] of Lin *et al*. [8]; Dashed lines: this study based on the K_S and its pressure derivative of MgO with the density of $(Mg_{0.75},Fe_{0.25})O$ [11,23]; Dash-dotted lines: V_P, V_S, and G of MgO [23]; Dotted lines: $(Mg_{0.94},Fe_{0.06})O$ from Brillouin measurements [12]; Solid lines: $(Mg_{0.83},Fe_{0.17})O$ from previous ultrasonic measurements [2]; Open squares: V_P, V_S , and G of single-crystal $(Mg_{0.76},Fe_{0.24})O$ at ambient conditions from previous ultrasonic measurements [3]. Errors are based on the statistics of the data, and some error bars are smaller than the symbol size.

Fig. 3. Elastic, thermodynamic, and vibrational parameters as a function of pressure obtained from integration of the PDOS [20]. (A): mean force constant, D_{av}; (B): Lamb-Mössbauer factor, f_{LM}; (C): vibrational specific heat, C_{vib} (k_B, Boltzmann constant); (D): vibrational entropy, S_{vib}; (E): kinetic energy at 0 K, E_Z; (F): kinetic energy, E_k. We note that these values only represent the contribution of the Fe sublattice in $(Mg_{0.75},Fe_{0.25})O$.

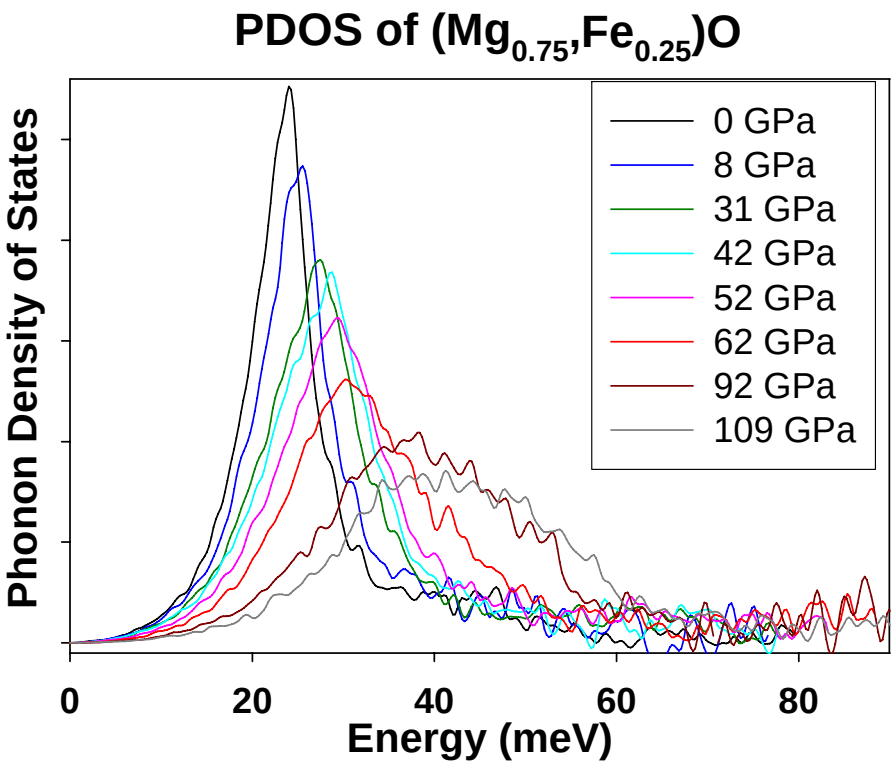
PDOS of (Mg0.75,Fe0.25)O
Phonon Density of States
0 GPa
8 GPa
31 GPa
42 GPa
52 GPa
62 GPa
92 GPa
109 GPa
0
20
40
60
80
Energy (meV)

Fig. 1

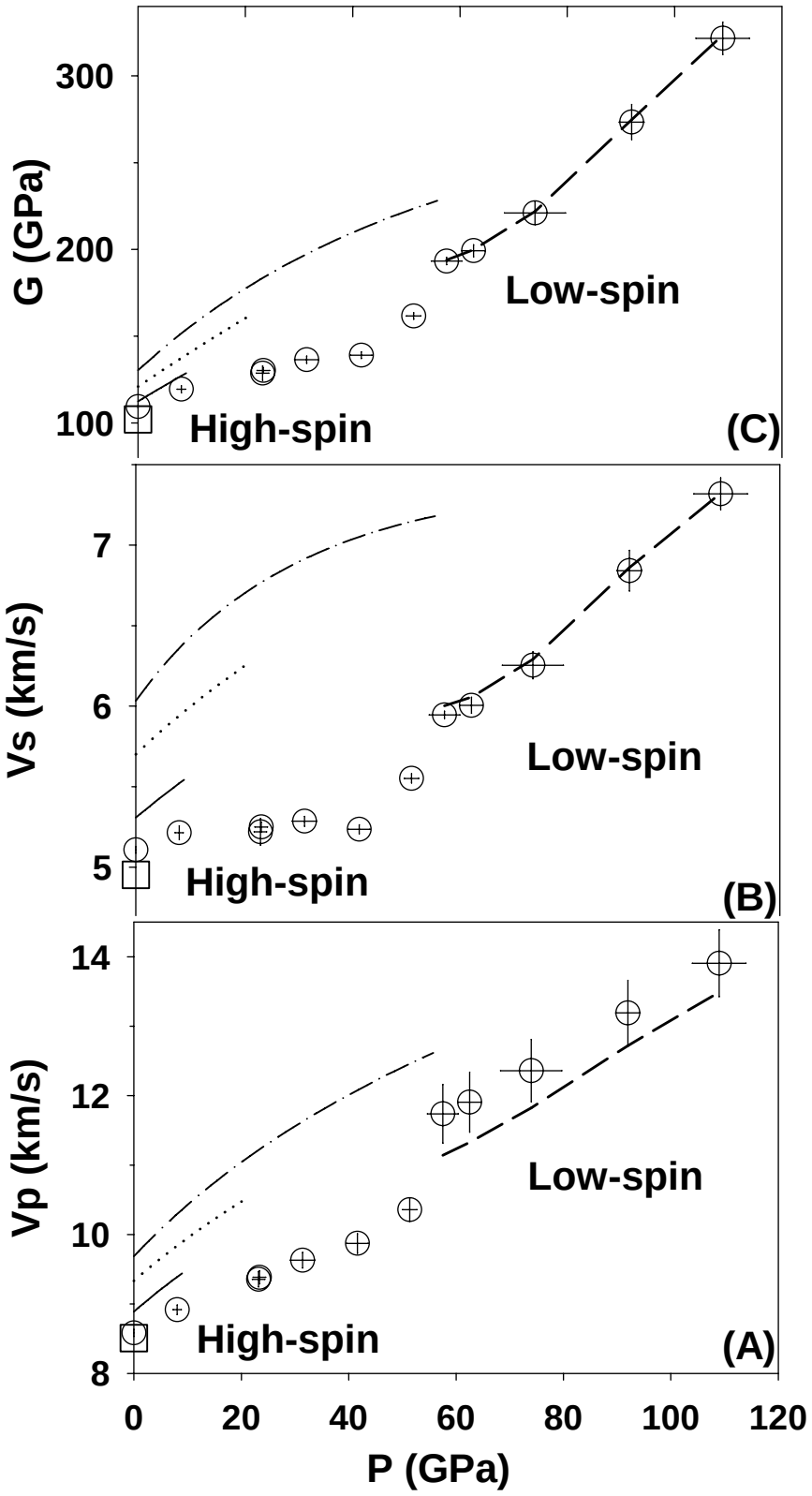
G (GPa)
300
200
100
Low-spin
High-spin
(C)
Vs (km/s)
7
6
5
Low-spin
High-spin
(B)
Vp (km/s)
14
12
10
8
Low-spin
High-spin
(A)
0
20
40
60
80
100
120
P (GPa)

Fig. 2

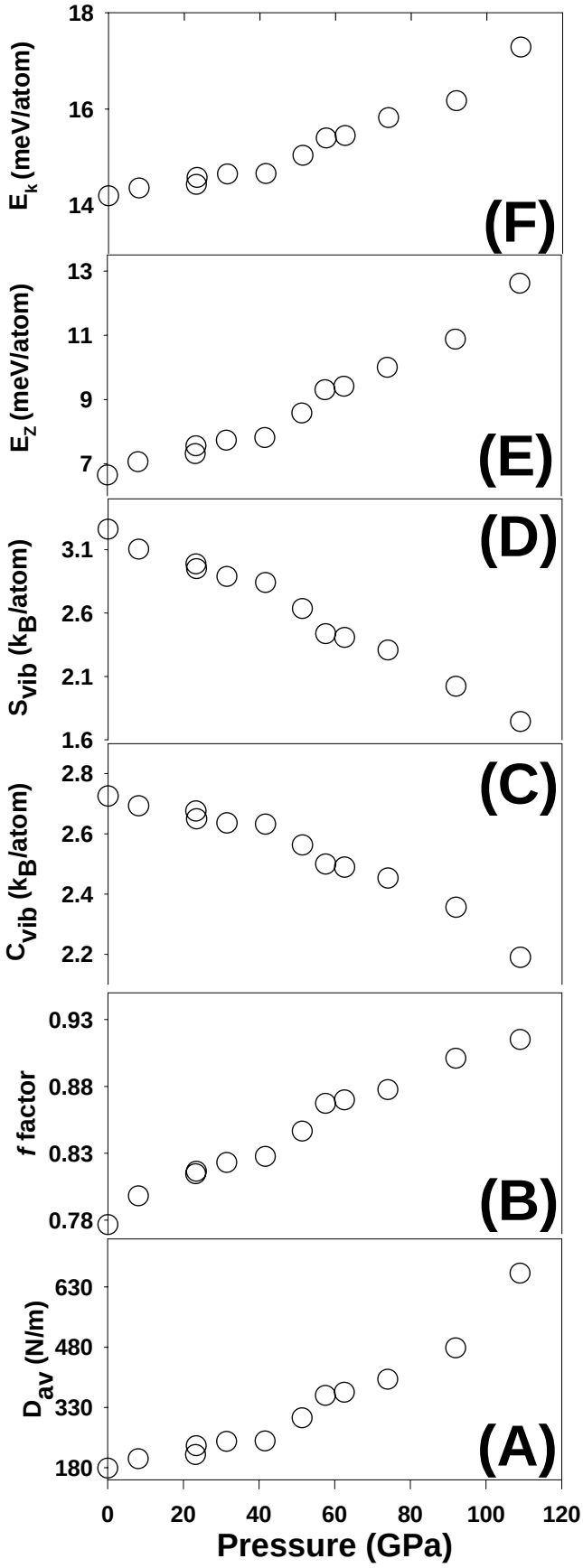
18
16
14
E_k (meV/atom)
(F)
13
11
9
7
E_Z (meV/atom)
(E)
3.1
2.6
2.1
1.6
S_{vib} (k_B/atom)
(D)
2.8
2.6
2.4
2.2
C_{vib} (k_B/atom)
(C)
0.93
0.88
0.83
0.78
f factor
(B)
630
480
330
180
D_{av} (N/m)
(A)
0
20
40
60
80
100
120
Pressure (GPa)

Fig. 3

Supporting Online Material

Materials and Methods:

Polycrystalline $(Mg_{0.75},Fe_{0.25})O$ with ~95% enrichment in ^{57}Fe was synthesized in an oxygen fugacity controlled gas-mixing furnace [S1,S2]. X-ray diffraction and Mössbauer spectra of the sample indicate the sample was free of magnetite (Fe_3O_4) contamination and the Fe^{3+} content was below detection levels of ~1%. For experiments below 33 GPa, the sample was loaded into the sample chamber of a DAC with a neon pressure medium and a few ruby balls. For experiments above 33 GPa, a perforated diamond [S3] having 100 μm inner culet, 300 μm outer culet, and a bevel angle of 9 degrees on the side of the incident X-ray beam was used to reduce absorption by the anvil, allowing NRIXS spectra to be collected within a reasonable time frame of less than a day. A beryllium gasket of 3 mm in diameter was pre-indented to a thickness of 30 μm and a hole of 250 μm was drilled in it. Subsequently, amorphous boron powder was inserted into the drilled hole and a smaller hole of 50 μm in diameter was drilled and used as the sample chamber. Use of the boron gasket insert helps to strengthen the Be gasket, increase the sample volume, and reduce the axial pressure gradients [S4]. The very small and highly focused X-ray beam of less than 10 μm in diameter also helps to reduce the pressure uncertainty caused by the radial pressure gradient. Pressures were determined using the ruby fluorescence scale [S5], and the pressure uncertainty (1σ) was estimated from multiple pressure measurements from the ruby balls in the sample chamber.

The adiabatic bulk modulus (K_S), density (ρ), and bulk Debye sound velocity (V_D) are used to solve for the aggregate V_P, V_S, and G by the following equations [S6]:

$$\frac{K_S}{\rho} = V_P^2 - \frac{4}{3}V_S^2 \quad (1)$$

$$\frac{G}{\rho} = V_S^2 \quad (2)$$

$$\frac{3}{V_D^3} = \frac{1}{V_P^3} + \frac{2}{V_S^3} \quad (3)$$

STable 1 Elastic, vibrational, and thermodynamic parameters of $(Mg_{0.75},Fe_{0.25})O$ obtained from the NRIXS study in a DAC. Adiabatic bulk modulus, K_S; compressional wave velocity, V_P; shear wave velocity, V_S; shear modulus, G; mean force constant, D_{av}; Lamb-Mössbauer factor, f_{LM}; vibrational specific heat, C_{vib} (k_B, Boltzmann constant); vibrational entropy, S_{vib}; kinetic energy, E_k; kinetic energy at T=0, E_Z . Errors are based on the statistics of the data. Under ambient conditions, the thermoelastic parameters for $(Mg_{0.76},Fe_{0.24})O$ by ultrasonic measurements under ambient conditions [S7] are: K_S=165 ($\pm$2) GPa, G=102 ($\pm$3), V_P=8.51 ($\pm$0.09) km/s, and V_S; =4.95 ($\pm$0.08), consistent with our study and verifying the procedure for deriving sound velocities from PDOS

P (GPa)	Ks (GPa)	Vp (km/s)	Vs (km/s)	G (GPa)	D_{av} (N/m)	f_{LM}	C_{vib} (k_B/atom)	S_{vib} (k_B/atom)	E_k (meV/atom)	E_Z (meV/atom)
	163.1	8.58	5.108	109.4	179	0.7767	2.725	3.262		
0	(3.8)	(0.05)	(0.020)	(0.9)	(6)	(0.0013)	(0.022)	(0.021)	14.20 (0.16)	6.65 (0.12)
8.06	190.0	8.92	5.214	119.4	202	0.7982	2.693	3.104		
(0.8)	(4.8)	(0.07)	(0.043)	(2.0)	(14)	(0.0020)	(0.037)	(0.030)	14.36 (0.31)	7.06 (0.25)
23.2	241.9	9.36	5.219	128.7	212	0.8146	2.676	2.987		
(1.2)	(8.3)	(0.11)	(0.082)	(4.1)	(21)	(0.0028)	(0.056)	(0.043)	14.43 (0.47)	7.32 (0.38)
23.4	242.5	9.38	5.250	130.3	234	0.8164	2.650	2.950		
(1.2)	(8.3)	(0.09)	(0.030)	(1.7)	(80	(0.0014)	(0.025)	(0.022)	14.58 (0.19)	7.56 (0.15)
31.4	271	9.63	5.285	136.5	245	0.8231	2.636	2.888		
(2.3)	(11)	(0.11)	(0.031)	(2.1)	(7)	(0.0013)	(0.023)	(0.020)	14.65 (0.18)	7.73 (0.14)
41.6	309	9.87	5.235	139.1	246	0.8276	2.632	2.840		
(2.0)	(14)	(0.14)	(0.028)	(1.9)	(9)	(0.0014)	(0.025)	(0.021)	14.66 (0.20)	7.81 (0.16)
51.4	347	10.36	5.552	161.6	304	0.8465	2.563	2.635		
(1.3)	(18)	(0.16)	(0.029)	(1.9)	(11)	(0.0013)	(0.024)	(0.019)	15.04 (0.22)	8.58 (0.18)
57.5	496	11.74	5.946	193.3	360	0.8672	2.499	2.437		
(2.9)	(55)	(0.42)	(0.022)	(2.0)	(9)	(0.0010)	(0.018)	(0.014)	15.40 (0.17)	9.30 (0.14)
62.5	518	11.91	6.005	199.2	368	0.8699	2.489	2.408		
(2.1)	(58)	(0.43)	(0.049)	(3.4)	(11)	(0.0013)	(0.023)	(0.018)	15.45 (0.21)	9.41 (0.17)
74.0	569	12.36	6.253	221.1	400	0.8775	2.453	2.308		
(5.7)	(73)	(0.45)	(0.084)	(6.6)	(13)	(0.0020)	(0.031)	(0.024)	15.82 (0.27)	10.00 (0.23)
92.1	651	13.19	6.842	273.4	478	0.9009	2.356	2.022		
(2.3)	(73)	(0.47)	(0.126)	(10.2)	(28)	(0.0018)	(0.034)	(0.022)	16.17 (0.43)	10.88 (0.39)
109.0	732	13.91	7.319	321.7	664	0.9149	2.189	1.743		
(5.0)	(82)	(0.48)	(0.099)	(9.3)	(20)	(0.0014)	(0.023)	(0.016)	17.28 (0.28)	12.62 (0.25)

References:

[S1] S. D. Jacobsen *et al., J. Geophys. Res.* **107**, B2, 10.1029/2001JB000490 (2002).

[S2] J. F. Lin *et al.,* submitted to *Phys. Rev. Lett.* (2006).

[S3] A. Dadashev, M. P. Pasternak, G. Kh. Rozenberg, *Rev. Sci. Instrum.* **72**, 2633 (2001).

[S4] J. F. Lin, J. Shu, H. K. Mao, R. J. Hemley, G. Shen, *Rev. Sci. Instrum.* **74,** 4732 (2003).

[S5] H. K. Mao, J. Xu, P. M. Bell, *J. Geophys. Res.* **91**, 4673(1986).

[S6] H. K. Mao *et al., Science* **292**, 914 (2001).

[S7] S. D. Jacobsen *et al., J. Geophys. Res.* **107**, B2, 10.1029/2001JB000490 (2002).